JBIC Journal of Biological Inorganic Chemistry
https://doi.org/10.1007/s00775-019-01691-0

ORIGINAL PAPER

Immobilization of tyrosinase on Fe_3O_4@Au core–shell nanoparticles as bio-probe for detection of dopamine, phenol and catechol

Elham Arkan[1] · **Changiz Karami**[1] · **Ronak Rafipur**[2]

Received: 30 April 2019 / Accepted: 14 July 2019

Abstract

An optical bio-probe based on the immobilized tyrosinase on the surface of Fe_3O_4@Au was described for the detection of dopamine, phenol and catechol. The prepared bio-probe (Fe_3O_4@Au@tyrosinase) was characterized by means such as TEM, SEM, VSM, DLS and TGA. In the presence of the bio-probe, the phenol, catechol and dopamine were converted to benzoquinone, o-quinone and dopaquinone, and the fluorescence spectra appeared at 308 nm, 329 nm and 336 nm with ex = 270 nm, respectively. However, by increasing the concentration of phenolic compounds in the bio-probe, the amount of products (benzoquinone, o-quinone and dopaquinone) was increased which was the reason for the increase in fluorescence intensity. Using this mechanism, a bio-probe was designed such that the intensity of the fluorescence spectra increased proportionally with the increase of the substrate concentrations after different time periods. The 0.003 mg/mL of tyrosinase was loaded on 1.65 mg/mL of the Fe_3O_4@Au. The highest performance for a bio-probe was demonstrated at room temperature and pH 6.8. By investigating the characteristics of the response of the bio-probe to different phenolic compounds, it was found that the bio-probe had a linear response in the concentration range 5.0–75.0 µM, 10.0–100.0 µM for phenol and dopamine and 50.0–500.0 M for catechol. The Michaelis–Menten constant (K_m) of the bio-probe was calculated as 0.6 µM. Finally, the bio-probe seems to be stable and efficient even after about 2 months.

Graphic abstract

A novel and easy method for the detection of dopamine, phenol and catechol by florescence that uses oxide capability to identify the phenolic compounds was introduced.

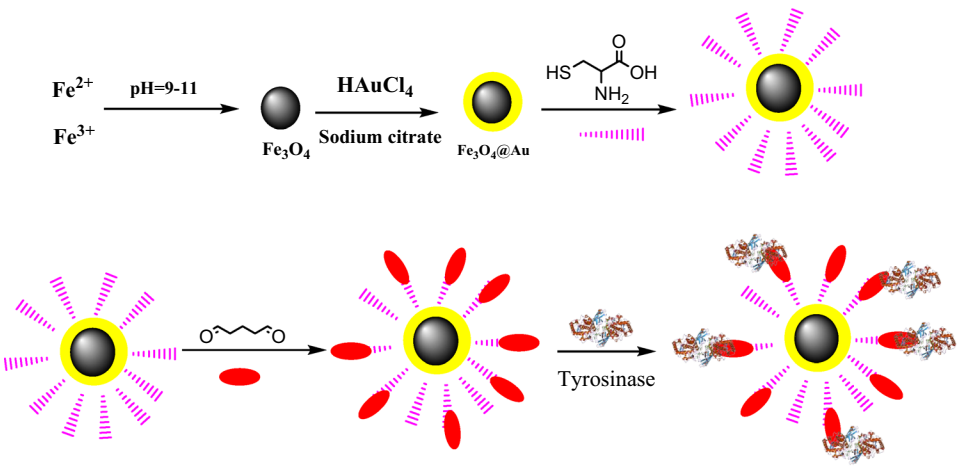

Keywords Fe_3O_4@Au · Optical sensor · Core–shell · Tyrosinase immobilization · Bio-probe · Dopamine · Phenol and catechol

Electronic supplementary material The online version of this article (https://doi.org/10.1007/s00775-019-01691-0) contains supplementary material, which is available to authorized users.

Extended author information available on the last page of the article

Published online: 29 July 2019

Introduction

One of the most critical constituents of hormones and neurotransmitters is the dopamine (DA) composition, which is a family of catecholamine and phenethylamine. Motivation, emotion, endocrine regulation, and locomotion are the essential roles of dopamine in the human body [1]. Regarding the usefulness of dopamine, the abnormal amount of dopamine causes a series of diseases, including schizophrenia and anorexia Parkinson's disease [2]. However, the amount of this compound in living organisms is between 0.1 and 10.0 mM, which is very low [3, 4]. Therefore, the measuring of dopamine amount for researchers is still interesting [5]. Catechol is another compound that causes a series of diseases in humans, animals, and plants, and its toxicity is dangerous because the skin quickly absorbs it [6, 7].

Another compound that is considered by researchers is phenol [8]. Phenol is one of the most common compounds that cause environmental contamination, and this compound as a corrosive compound is easily absorbed by contact with skin or by ingestion and inhalation. One of the disadvantages of phenol is that the amount of 21 μM is very toxic and dangerous to fish and the concentration between 106 and 1062 μM causes the death of the entire aquatic ecosystem [9, 10]. It is considering that the wide variety of sources are available for the production of phenol, including the refineries coal processing, coking operations, manufacture of petrochemicals, wood product, plastic, pharmaceutical, and paper industries, etc. However, it can be concluded that a large amount of this composition exists in the environment, including drinking water [11, 12]. Besides, the use of drinking water, with phenol, can lead to several diseases including diarrhea, nausea, dark urine, mouth sores, kidney damage and paralysis of the central nervous system [13]. The bioaccumulation of phenol in human and animal tissue and biomagnification in food chains can lead to severe contamination and hence is a significant concern [14].

So far, different methods for measuring dopamine have been introduced, such as mass spectrometry, high-performance liquid chromatography, and electrochemical techniques [15–17]. The same techniques, such as gas chromatography, capillary electrophoresis, and spectrophotometry analysis, are used to measure phenol [18, 19], but these techniques have a lot of drawbacks. For instance, gas chromatography and HPLC are time consuming, complicated and also involves expensive equipment. Among others, fluorescence-based methods are remarkable for researchers because this technique can detect trace amounts of analytes in various samples. Sensitivity, wide linear dynamic range, rapidity, high accuracy, and selectivity are the advantages of fluorescence methods that make it attractive to researchers [20–23].

In various fields of science, including drug delivery, pharmacy and biotechnology, the Fe_3O_4 magnetic nanoparticles are of interest to researchers which attributed to the low toxicity, biocompatibility, strong supermagnetism, catalytic activity, the ease of preparation, the ability to functionalize, and the separation of the product from the external magnetic field in the reaction [24–30].

Among different Fe_3O_4 magnetic structures, the Fe@Au (core–shell) structure is very important. The Au as an inert element is very suitable for coating magnetic nanoparticles, unique biocompatibility and versatility in surface modification [31]. Due to the noticeable advantages of Au nanoparticles, this core–shell ability has made it possible to modify biomolecules such as enzymes and use them as biosensors.

A lot of sensors were used [32–37]. Biosensors are introduced as an ideal system for monitoring phenolic structures due to high selectivity, fast response cost-effectiveness and simplicity of operation and manufacture. Known biomolecules such as tyrosinase [38], laccase [39] and horseradish peroxidase are used as biosensors and bio-probe to the detection of phenolic compounds [40]. The tyrosinase enzymes can catalyze reactions: the hydroxylation of monophenols to benzoquinone and the oxidation of o-diphenols to o-quinones [41]. However, due to limitations on the use of enzymes, the design of biosensors based on the immobilization of the tyrosinase enzyme is very much considered [42]. Several examples of immobilization methods such as incorporation within carbon paste [43], physical adsorption [44], immobilization in polymer films [45], and covalent cross-linking [46] have been reported. These methods had problems such as complicated synthesis, low stability, weak bioactivity maintenance, etc. Thus, the immobilization of the tyrosinase that does not have the issues listed above is a special challenge for researchers.

By considering the advantages of using the core–shell of iron–gold structure, in this research, the bio-probe of Fe_3O_4@tyrosinase was synthesized and characterized by several techniques such as TEM, FT-IR, SEM, TGA, VSM, and DLS. Proposed mechanism for this bio-probe, the compounds such as phenol, catechol and dopamine was oxidation and convert to benzoquinone, o-quinone and dopaquinone, respectively, in the presence of tyrosinase, and a new fluorescence spectrum at 308 nm, 329 nm and 336 nm, respectively, was appeared. By increasing the concentration of each of these compounds into the specified amount of Fe_3O_4@tyrosinase, the fluorescence spectrum increased. Thus, by linking the spectrum of fluorescence to the phenol concentration of 308 nm, catechol at 329 nm and dopamine at 336 nm, a bio-probe can be designed to detect phenol, catechol and dopamine. Finally, to evaluate the best conditions, the parameters such as time, temperature and pH of the reaction were also investigated.

Experimental

Reagents

The chemical materials such as tyrosinase (from mushroom 2067 units/mg), glutaraldehyde (2.5%), *N*-hydroxysuccinimide (NHS), $FeCl_2$ $4H_2O$, 99%, and $FeCl_3$ $6H_2O$, 99% EDC (1-ethyl-3-(3-dimethylaminopropyl)carbodiimide) were purchased from Sigma-Aldrich. Trisodium citrate dehydrates, ammonium hydroxide, $HAuCl_4.4H_2O$ (99.99%) and glutaraldehyde (25% water solution) were purchased from Merck.

Apparatus and measurements

For the functional group properties of the bio-probe, the FT-IR spectra were recorded in the wavenumber range 400–4000 cm^{-1} [Thermo (AVATAR)]; the surface morphology of nanoparticle was studied by scanning electron microscope (SEM) (TESCAN, MIRA III). The particles were measured by the TEM (JEOL-JEM 2010). The value of the magnetic properties was studied using the vibrating sample magnetometer (VSM, LakeShore 7073). The dynamic light scattering (DLS) was used for hydrodynamic diameter (DLS, Malvern, and ZEN3600). Thermal gravimetric analysis (TGA–DTA) was another technique used to characterize the thermal stability of compounds (Germany, Bahr, STA504).

Immobilization of tyrosinase

For immobilization of the tyrosinase on the Fe_3O_4@Au@cysteine, the Fe_3O_4@Au@cysteine was modified using glutaraldehyde as a cross-linking reagent. Fe_3O_4@Au@cysteine (20 mg) was added to 1.0 ml of glutaraldehyde (2.5%) under the agitation at room temperature for 3 h, and the mixture was centrifuged and the product was washed with PBS four times. Then the tyrosinase (5.0 mg $mL^{-1)}$ was added to Fe_3O_4@Au@cysteine with 5.0 ml of PBS (pH 6.8), and the mixture was agitated for 24 h at 4 °C. The precipitates were washed by PBS for the removal of excess tyrosinase. The formed magnetic bio-nanoparticles were stored at 4 °C in a refrigerator. The synthesis of the Fe_3O_4 and Fe_3O_4@Au@cysteine was described in the supporting information (SI) [47].

Detection of DA, phenol and catechol

1.65 mg/mL of freshly prepared bio-nanoparticles was mixed with different concentrations (10.0–100 µM) of DA solutions, (5.0–75.0 µM) phenol solutions and (50.0–500 µM) catechol. Then with PBS (pH 6.8) the solution was diluted to 1.0 mL and incubated for 15 min for DA, 5 min for phenol and 10 min for catechol at ambient temperature. In the excitation wavelength at 270 nm, the fluorescence spectra were recorded at 308 nm for phenol, 329 nm for catechol and 336 nm for dopamine. The slit widths were 5 nm and 15 nm for ex/em.

Activity assays of tyrosinase

The Bradford method was used to calculate the amount of immobilized tyrosinase on the Fe_3O_4@Au@tyrosinase, The concentration of bovine albumin as a protein standard was measured using the Bradford method. This testing was carried out at ambient temperature. The optimum enzyme loading on 1.65 mg/mL of the Fe_3O_4@Au core–shell was found to be 0.003 mg/mL [48].

Results and discussion

Characterization of bio-nanoparticles

The TEM and SEM were used for the characterization of particle size and surface morphology of Fe_3O_4@Au@tyrosinase, the FT-IR was used for functional groups, the DLS, VSM and TGA methods also were used for particle size, magnetic properties and stability of the bio-probe, respectively. The FT-IR spectra of bare Fe_3O_4, Fe_3O_4@Au@cysteine and Fe_3O_4@tyrosinase are shown in Fig. 1. The peak observed at 585 cm^{-1} is attributed to the Fe–O bond vibration and the broadband peak at 3300–3500 cm^{-1} is attributed to the O–H stretching vibrations (Fig. 1a). The peak band at approximately 3422 cm^{-1} is attributed to OH stretching vibration and peak at 2973–2893 cm^{-1} is related to the stretching vibration of C–H bond. In Fe_3O_4@Au@cysteine, the peak at 3423 cm^{-1} is attributed to the N–H

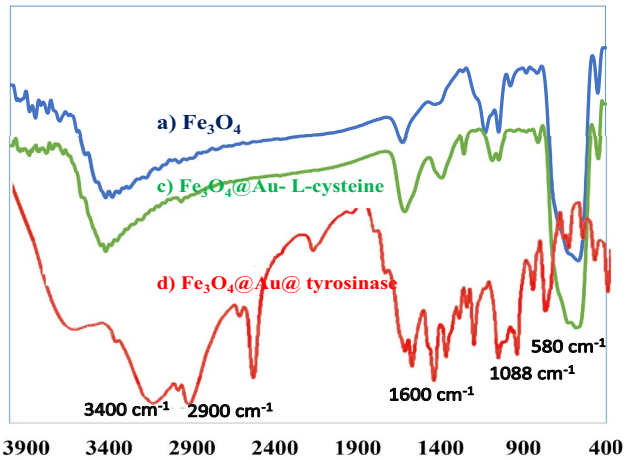

Fig. 1 The FT-IR spectra of *a* the Fe_3O_4 nanoparticles, *b* Fe_3O_4@Au@cysteine, and *c* Fe_3O_4@tyrosinase

stretching vibrations of amine group NH_2 and signals at 2924 and 2968 cm^{-1} are related to the symmetric and asymmetric vibrations of the C–H bond, and 16,354 cm^{-1} corresponds to the stretching vibration of the carbonyl group (Fig. 1b). To show the presence of enzymes on the surface of the Fe_3O_4@ Au@cysteine, the main peaks at 1571 cm^{-1}, 1405 cm^{-1} and 3295 cm^{-1} related to secondary amide and hydroxyl groups, respectively. Therefore, the FT-IR results provide evidential component information of differently modified Fe_3O_4.

The SEM image of bio-nanoparticles is shown in Fig. 2a which shows the particles have a spherical shape with 30 nm diameter. Also, the TEM image shows the spherical shape and diameter of the particle (30 nm) (Fig. 2b) and shows the thickness of the Au around the core which is about 0.8 nm.

The magnetic properties of the bio-probe are shown in Fig. 3. Figure 3a, b shows the values of the saturation magnetization of the Fe_3O_4 and Fe_3O_4@Au@tyrosinase which are 63.5 and 48.5 emu/g, respectively. A significant decrease in the magnetic property of Fe_3O_4@Au@tyrosinase in comparison to the Fe_3O_4 state is due to layers such as cysteine, tyrosinase and diamagnetic Au. Anyway, Fig. 3c, is shown, the Fe_3O_4@Au@tyrosinase is separated with an external magnet at 5 min, and this decreases the magnetic strength does not have much effect on the separation of the bio-probe from the solution. The TGA of the Fe_3O_4 and Fe_3O_4@Au@tyrosinase at 15 °C/min under nitrogen atmosphere was done (Fig. 4). The TGA curve (a) is related to the as-prepared Fe_3O_4; at 225–250 °C, it loses significant weight (5%) which is due to the dehydroxylation of Fe–O in the Fe_3O_4

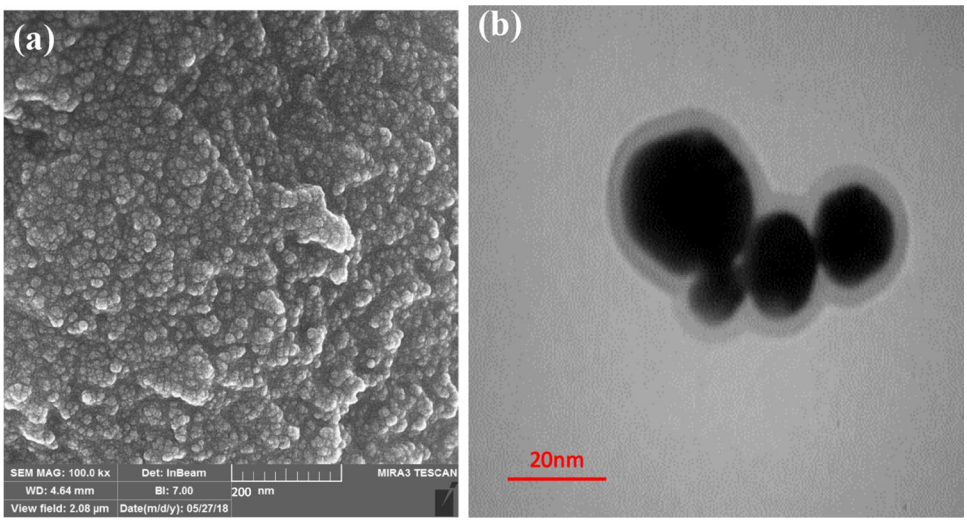

Fig. 2 **a** SEM image of Fe_3O_4@Au@tyrosinase and **b** TEM image of Fe_3O_4@Au@tyrosinase

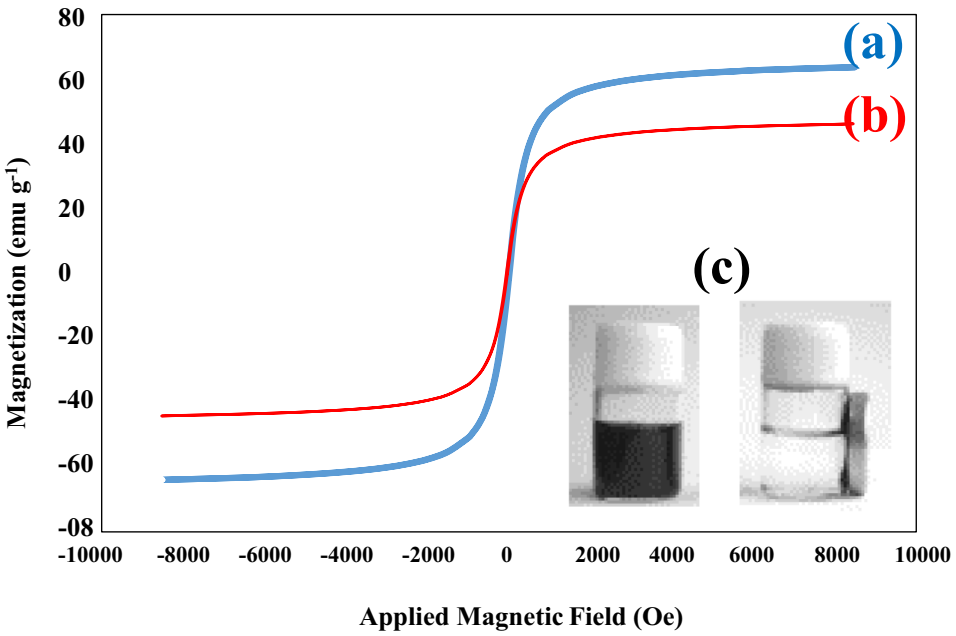

Fig. 3 Magnetization curves of *a* Fe_3O_4 and *b* Fe_3O_4@Au@cysteine. *c* The photographs of Fe_3O_4@Au@tyrosinase dispersed in solution (left), and separated from water solution under an external magnetic field (right)

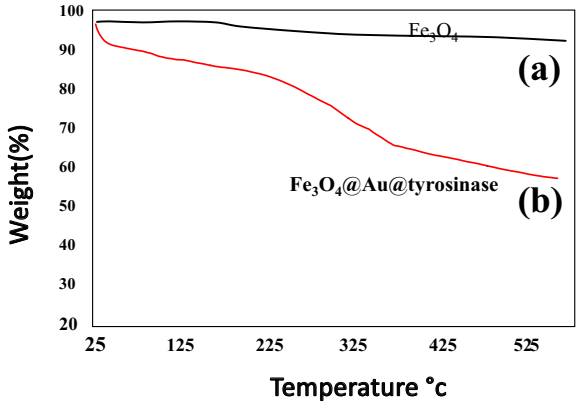

Fig. 4 The TGA curves of *a* Fe_3O_4 and *b* Fe_3O_4@Au@cysteine

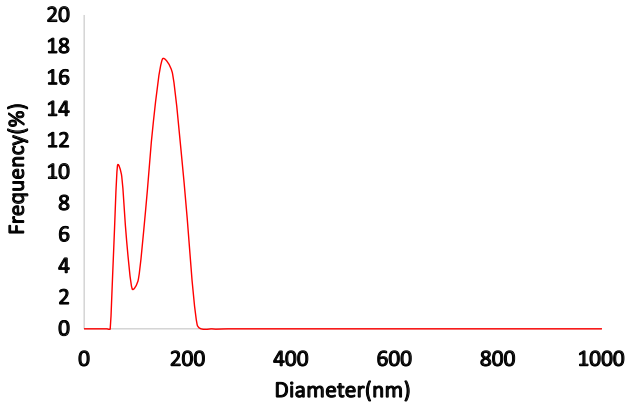

Fig. 5 The particle size by DLS with PI = 0.313

structure [49]. In curve (b), weight loss occurs in several steps, the first step until 100 ℃ is about 10% weight that is related to the adsorbed physical and chemical water. In the next step that starts at 100 °C until 225 °C is related to the de-hydroxylation of Fe–O structure, it is losing about 20% of its weight. The last step that starts at 225 °C until 600 °C is due to the decomposition of other functional groups such as carboxyl and hydroxyl of tyrosinase. The TGA curves of Fe_3O_4@Au@tyrosinase pointed that coated layer of Fe_3O_4 is about 58%. Figure 5 shows the particle size of Fe_3O_4@Au@tyrosinase by a DLS, the particle size in a DLS is 100 nm which is larger than the TEM in comparison. In the explanation of the difference of particle size between DLS and TEM, the TEM image is related to the metal core (Fe and Au) while the DLS contains a metallic core plus the layers of the organic ligand such as glutaraldehyde, cysteine and tyrosinase.

Possible mechanism of the bio-sensing

The basic principle of Fe_3O_4@Au@tyrosinase detection of DA, phenol and catechol is illustrated in Scheme 1. Considering that the tyrosinase on the surface of bio-probe was used, and due to the high ability of this enzyme to oxidize phenolic compounds, the basis for detection was based on the ability to oxidize phenolic compounds by tyrosinase. In the presence of the bio-probe, dopamine, phenol and catechol converted to dopaquinone, benzoquinone and o-quinone, respectively [50, 51]. For each of these products (benzoquinone, dopaquinone, and quinone), a fluorescence spectrum appeared at 308 nm, 336 nm and 329 nm with ex = 270 nm. However, by increasing the concentration of dopamine, phenol and catechol to the bio-probe, the amount of dopaquinone, benzoquinone and o-quinone as a product in the solution increases, so the fluorescence intensity was increased. Using these data, a bio-probe can be designed such that the increase in fluorescence intensity related to increasing the concentration of dopamine, phenol and catechol (Fig. 6).

Scheme 1 Different stages of the synthesis of Fe_3O_4@Au@tyrosinase

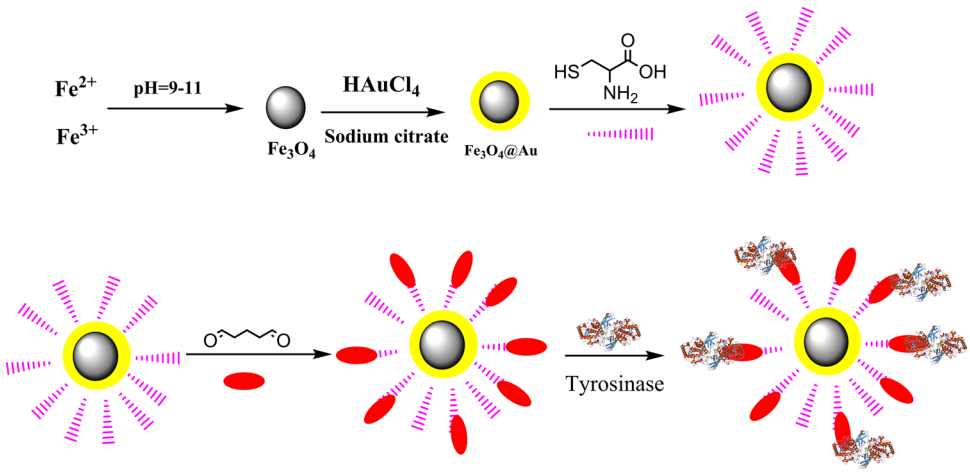

Optimization of the experimental conditions

The optimal conditions for this kind of bio-probes are very important. The optimal conditions for this kind of bio-probes are very important because tyrosinase activity is highly dependent on pH. As you well know, various enzymes require different times for their reaction as a catalyst. Nonetheless, the effects of different pH values (3, 4, 6, 6.5 and 6.8) for the detection of DA, phenol and catechol were investigated, and the fluorescence intensities at 336 nm, 308 nm and 329 nm for these pHs were calculated. Given the highest performance of the bio-probe, the highest amount of DA, phenol and catechol was oxidized. Therefore, the best-optimized condition was for a situation that the fluorescence spectrum had a low intensity in the spectrum. Therefore, to continue measuring DA, phenol and catechol, the phosphate buffer at pH 6.8 was used (Figs. S1, S2, S3).

As you know, various enzymes require different times for their reaction as a catalyst. To obtain the best reaction time in this system, the fluorescence intensity was calculated with a mixture of Fe_3O_4@Au@tyrosinase and the DA, phenol and catechol at different times from 1 min to 30 min. In Figs. S3, S4, and S5, it can be seen that by increasing the reaction time to 5 min for phenol, 15 min for DA and 10 min for catechol, the fluorescence intensity decreases, and after this time the fluorescence intensity reduction can be neglected. Nevertheless, the favorable conditions for these reactions were 5 min for phenol, 15 min for DA and 10 min for catechol with a pH 6.8 of phosphate buffer.

Calibration curves and detection limit

The bio-probe performance in the detection of phenolic compounds (DA, phenol and catechol) under the optimized experimental conditions was studied. For this purpose, the wavelengths of 336, 308 and 329 nm were chosen (ex = 270 nm) for the respective determination of DA, phenol and catechol, respectively. As shown in Fig. 7, the intensity of the fluorescence spectra with various concentration ranges of phenolic compounds had different performances. The fluorescence intensity of concentration of the dopamine (DA) in the presence of bio-probe was linear over the range 10.0–100.0 µM with a calibration equation of $y = 5.503x + 107.96$ ($r = 0.96$) (Fig. 7a), and 5.0–75.0 µM range with a calibration equation of $y = 8.44x + 338.95$ ($r = 0.9805$) for phenol (Fig. 7b). For catechol, a wide range (50.0–500 µM) with a calibration equation of $y = 1.51x + 235.5$ ($r = 0.99$) was calculated (Fig. 7c). The detection limit of 1.00 µM for DA, 5.00 µM for phenol and 20.00 µM for catechol was obtained ($S/N = 3$).

For activity, the Michaelis–Menten constant (K_m) was calculated from the Lineweaver–Burk equation:

$$1/V_{ss} = (K_m/V_{max}) \times 1/[C] + (1/V_{max}), \quad (1)$$

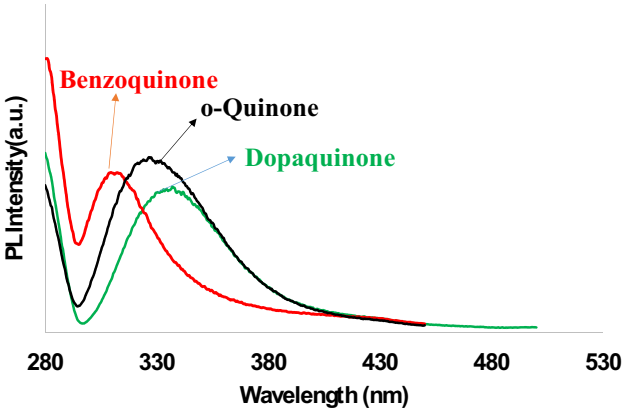

Fig. 6 The emission spectrum of DA, phenol and catechol in the presence of magnetic bio-probe in the experiment (ex = 270 nm)

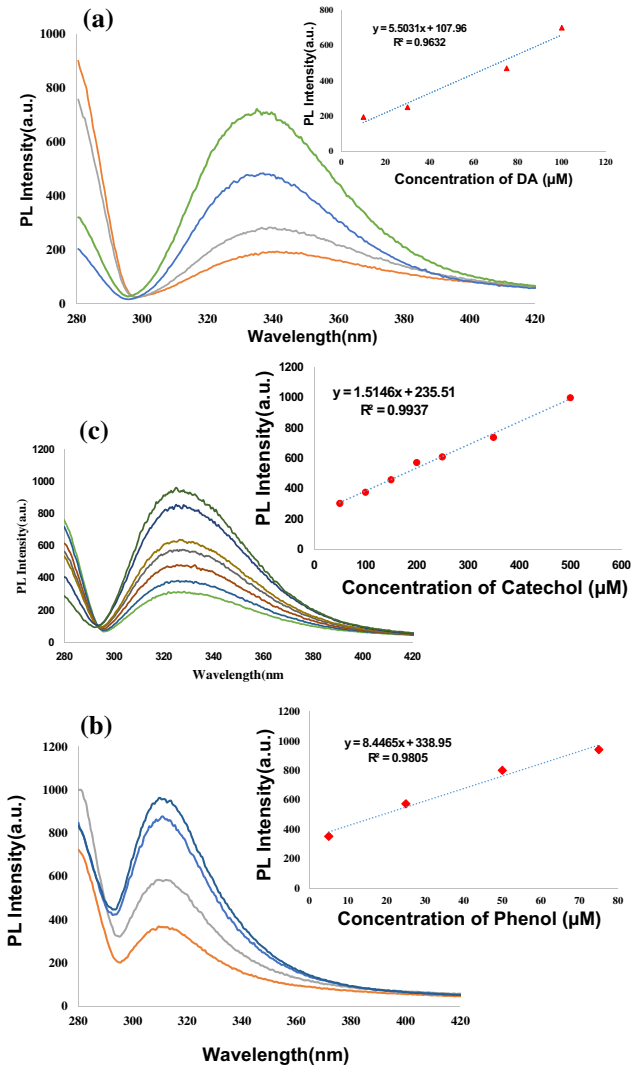

Fig. 7 The response curve of the biosensor towards **a** DA, **b** phenol and **c** catechol in the different range, pH 6.8, **b** Increase in the relative sensitivity of the detection system concerning the concentration of the DA, phenol and catechol

where V_{ss} is the steady-state current, K_m is the Michaelis–Menten constant, V_{max} is the maximum current of the reaction and C is the concentration of the substrate. K_m was 0.6 µM, and V_{max} was 6.8 µM/min. The calculated K_m was lower than previous research [7, 42] which indicates that this enzyme has higher phenolic compound affinity.

Selectivity and interferences

The oxidation products of phenol, dopamine and catechol had specific wavelength at ex = 270 nm; however, the selectivity of the technique was examined with other molecules such as uric acid (UA), glucose (Glc), inositol (Ins), amino acids such as Ala, Gln, Cys, Arg, Glu, Leu, Ile, Trp and Lys), and some ions such as Mg^{2+}, Na^{+}, Ca^{2+}, and K^{+}). In Fig. S6, it is seen that the fluorescence spectrum at ex = 270 nm does not appear; therefore, this system is not selective for the above materials. For the study of interferences, Fig. S7 clearly shows phenolic compounds (phenol, dopamine and catechol) with the compounds mentioned above not interfering with the results of the proposed method even if they were present at 100-fold higher concentrations.

Real sample analysis

To evaluate the real sample analysis of the proposed method, the human serum samples were collected from healthy volunteers and diluted tenfold by PBS (pH 6.8) before. The known concentrations of DA, phenol or catechol were spiked to diluted human serums and detected under the optimum conditions. As shown in Table 1, the results fully agree with the spiked values. These results suggest that matrix effects from the diluted serum did not affect the substantial detection.

Conclusion

A favorable method of immobilized tyrosinase in a Fe_3O_4@Au core–shell for the development of an optical bio-probe of dopamine, phenol and catechol has been described based on the oxidation of the phenolic compounds in the presence of tyrosinase. By increasing the substrate concentration, the fluorescence intensity was increased proportionally. The bio-probe permits good sensitivity and stability. The LOD towards DA, phenol and catechol was observed to be 1.00 µM for DA, 5.00 µM for phenol and 20.00 µM ($S/N = 3$). Eventually, the developed bio-probe has good potential for determining the amount of dopamine, phenol and catechol in human serum.

Table 1 Determination of concentration amounts of DA, phenol or catechol in serum samples ($n = 3$)

Sample		Added (µM)	Found (µM)	Recovery (%)	RSD%
DA	1	0	–	–	–
	2	10	9.9	99	5.1
	3	20	21	105	4.76
	4	50	54.3	108	2.8
Phenol	1	0	–	–	–
	2	10	10.4	104	5.7
	3	20	19.8	99	5.2
	4	50	53.6	101.2	3.87
Catechol	1	0	–	–	–
	2	50	52.1	100.2	1.4
	3	100	103	103	4.2

Acknowledgements The authors gratefully acknowledge the Research Council of Kermanshah University of Medical Sciences (Grant number: 97708) for the financial support.

References

1. Liggett SB (2000) Pharmacogenetics of beta-1-and beta-2-adrenergic receptors. Pharmacology 61(3):167
2. Jaber M, Robinson SW, Missale C, Caron MG (1996) Dopamine receptors and brain function. Neuropharmacology 35(11):1503–1519
3. Ali SR, Ma Y, Parajuli RR, Balogun Y, Lai WY-C, He H (2007) A nonoxidative sensor based on a self-doped polyaniline/carbon nanotube composite for sensitive and selective detection of the neurotransmitter dopamine. Anal Chem 79(6):2583–2587
4. Ankireddy SR, Kim J (2015) Selective detection of dopamine in the presence of ascorbic acid via fluorescence quenching of InP/ZnS quantum dots. Int J Nanomed 10(1):113
5. He Y-S, Pan C-G, Cao H-X, Yue M-Z, Wang L, Liang G-X (2018) Highly sensitive and selective dual-emission ratiometric fluorescence detection of dopamine based on carbon dots-gold nanoclusters hybrid. Sens Actuators B Chem 265:371–377
6. Freire RS, Durán N, Kubota LT (2002) Electrochemical biosensor-based devices for continuous phenols monitoring in environmental matrices. J Braz Chem Soc 13(4):456–462
7. Leboukh S, Gouzi H, Coradin T, Yahia H (2018) An optical catechol biosensor based on a desert truffle tyrosinase extract immobilized into a sol–gel silica layered matrix. J Sol-Gel Sci Technol 86(3):675–681
8. Gupta VK, Karimi-Maleh H, Sadegh R (2015) Simultaneous determination of hydroxylamine, phenol and sulfite in water and waste water samples using a voltammetric nanosensor. Int J Electrochem Sci 10:303–316
9. Huang J, Wang X, Jin Q, Liu Y, Wang Y (2007) Removal of phenol from aqueous solution by adsorption onto OTMAC-modified attapulgite. J Environ Manag 84(2):229–236
10. Contreras EM, Albertario ME, Bertola NC, Zaritzky NE (2008) Modelling phenol biodegradation by activated sludges evaluated through respirometric techniques. J Hazard Mater 158(2–3):366–374

11. Busca G, Berardinelli S, Resini C, Arrighi L (2008) Technologies for the removal of phenol from fluid streams: a short review of recent developments. J Hazard Mater 160(2–3):265–288
12. Wei G, Yu J, Zhu Y, Chen W, Wang L (2008) Characterization of phenol degradation by Rhizobium sp. CCNWTB 701 isolated from *Astragalus chrysopteru* in mining tailing region. J Hazard Mater 151(1):111–117
13. Senturk HB, Ozdes D, Gundogdu A, Duran C, Soylak M (2009) Removal of phenol from aqueous solutions by adsorption onto organomodified Tirebolu bentonite: equilibrium, kinetic and thermodynamic study. J Hazard Mater 172(1):353–362
14. dos Santos VL, de Souza Monteiro A, Braga DT, Santoro MM (2009) Phenol degradation by *Aureobasidium pullulans* FE13 isolated from industrial effluents. J Hazard Mater 161(2–3):1413–1420
15. van de Merbel NC, Hendriks G, Imbos R, Tuunainen J, Rouru J, Nikkanen H (2011) Quantitative determination of free and total dopamine in human plasma by LC–MS/MS: the importance of sample preparation. Bioanalysis 3(17):1949–1961
16. Perry M, Li Q, Kennedy RT (2009) Review of recent advances in analytical techniques for the determination of neurotransmitters. Anal Chim Acta 653(1):1–22
17. Mao Y, Bao Y, Gan S, Li F, Niu L (2011) Electrochemical sensor for dopamine based on a novel graphene-molecular imprinted polymers composite recognition element. Biosens Bioelectron 28(1):291–297
18. Wang C, Wu C, Zhang L, Zhang J (2016) Ultraperformance liquid chromatography–tandem mass spectrometry method for profiling ketolic and phenolic sex steroids using an automated injection program combined with diverter valve switch and step analysis. Anal Chem 88(16):7878–7884
19. Quynh BTP, Byun JY, Kim SH (2015) Non-enzymatic amperometric detection of phenol and catechol using nanoporous gold. Sens Actuators B Chem 221:191–200
20. Gupta VK, Mergu N, Kumawat LK, Singh AK (2015) Selective naked-eye detection of magnesium (II) ions using a coumarin-derived fluorescent probe. Sens Actuators B Chem 207:216–223
21. Gupta VK, Mergu N, Kumawat LK, Singh AK (2015) A reversible fluorescence "off–on–off" sensor for sequential detection of aluminum and acetate/fluoride ions. Talanta 144:80–89
22. Yola ML, Gupta VK, Eren T, Şen AE, Atar N (2014) A novel electro analytical nanosensor based on graphene oxide/silver nanoparticles for simultaneous determination of quercetin and morin. Electrochim Acta 120:204–211
23. Gupta VK, Singh AK, Kumawat LK (2014) Thiazole Schiff base turn-on fluorescent chemosensor for Al3 + ion. Sens Actuators B Chem 195:98–108
24. Xing Y, Jin Y-Y, Si J-C, Peng M-L, Wang X-F, Chen C, Cui Y-L (2015) Controllable synthesis and characterization of Fe3O4/Au composite nanoparticles. J Magn Magn Mater 380:150–156
25. Zhang T, Wang W, Zhang D, Zhang X, Ma Y, Zhou Y, Qi L (2010) Biotemplated synthesis of gold nanoparticle–bacteria cellulose nanofiber nanocomposites and their application in biosensing. Adv Funct Mater 20(7):1152–1160
26. Lai G-S, Zhang H-L, Han D-Y (2009) Amperometric hydrogen peroxide biosensor based on the immobilization of horseradish peroxidase by carbon-coated iron nanoparticles in combination with chitosan and cross-linking of glutaraldehyde. Microchim Acta 165(1–2):159–165
27. Guo S, Li D, Zhang L, Li J, Wang E (2009) Monodisperse mesoporous superparamagnetic single-crystal magnetite nanoparticles for drug delivery. Biomaterials 30(10):1881–1889
28. Pham TTH, Cao C, Sim SJ (2008) Application of citrate-stabilized gold-coated ferric oxide composite nanoparticles for biological separations. J Magn Magn Mater 320(15):2049–2055
29. Kim J, Park S, Lee JE, Jin SM, Lee JH, Lee IS, Yang I, Kim JS, Kim SK, Cho MH (2006) Designed fabrication of multifunctional magnetic gold nanoshells and their application to magnetic resonance imaging and photothermal therapy. Angew Chem 118(46):7918–7922
30. Baby TT, Ramaprabhu S (2010) SiO2 coated Fe3O4 magnetic nanoparticle dispersed multiwalled carbon nanotubes based amperometric glucose biosensor. Talanta 80(5):2016–2022
31. Grabar KC, Freeman RG, Hommer MB, Natan MJ (1995) Preparation and characterization of Au colloid monolayers. Anal Chem 67(4):735–743
32. Dehghani MH, Sanaei D, Ali I, Bhatnagar A (2016) Removal of chromium (VI) from aqueous solution using treated waste newspaper as a low-cost adsorbent: kinetic modeling and isotherm studies. J Mol Liq 215:671–679
33. Karimi-Maleh H, Tahernejad-Javazmi F, Atar N, Yola ML, Gupta VK, Ensafi AA (2015) A novel DNA biosensor based on a pencil graphite electrode modified with polypyrrole/functionalized multiwalled carbon nanotubes for determination of 6-mercaptopurine anticancer drug. Ind Eng Chem Res 54(14):3634–3639
34. Asfaram A, Ghaedi M, Agarwal S, Tyagi I, Gupta VK (2015) Removal of basic dye Auramine-O by ZnS: Cu nanoparticles loaded on activated carbon: optimization of parameters using response surface methodology with central composite design. RSC Adv 5(24):18438–18450
35. Gupta KV, Nayak A, Agarwal S, Singhal B (2011) Recent advances on potentiometric membrane sensors for pharmaceutical analysis. Comb Chem High Throughput Screening 14(4):284–302
36. Vinod K (1995) Determination of lead using a poly (vinyl chloride)-based crown ether membrane. Analyst 120(2):495–498
37. Jain AK, Gupta VK, Sahoo BB, Singh LP (1995) Copper (II)-selective electrodes based on macrocyclic compounds. Analytical proceedings including analytical communications, vol 3. Royal Society of Chemistry, UK, pp 99–101
38. Yang L, Xiong H, Zhang X, Wang S (2012) A novel tyrosinase biosensor based on chitosan-carbon-coated nickel nanocomposite film. Bioelectrochemistry 84:44–48
39. Quan D, Kim Y, Shin W (2004) Characterization of an amperometric laccase electrode covalently immobilized on platinum surface. J Electroanal Chem 561:181–189
40. Kafi A, Chen A (2009) A novel amperometric biosensor for the detection of nitrophenol. Talanta 79(1):97–102
41. Chen X, Cheng G, Dong S (2001) Amperometric tyrosinase biosensor based on a sol–gel-derived titanium oxide–copolymer composite matrix for detection of phenolic compounds. Analyst 126(10):1728–1732
42. Abdullah J, Ahmad M, Karuppiah N, Heng LY, Sidek H (2006) Immobilization of tyrosinase in chitosan film for an optical detection of phenol. Sens Actuators B Chem 114(2):604–609
43. Wang J, Fang L, Lopez D (1994) Amperometric biosensor for phenols based on a tyrosinase–graphite–epoxy biocomposite. Analyst 119(3):455–458
44. Hall GF, Best DJ, Turner AP (1988) Amperometric enzyme electrode for the determination of phenols in chloroform. Enzym Microb Technol 10(9):543–546
45. Cosnier S, Innocent C (1993) A new strategy for the construction of a tyrosinase-based amperometric phenol and o-diphenol sensor. Bioelectrochem Bioenerg 31(2):147–160
46. Önnerfjord P, Emnéus J, Marko-Varga G, Gorton L, Ortega F, Domínguez E (1995) Tyrosinase graphite-epoxy based composite electrodes for detection of phenols. Biosens Bioelectron 10(6–7):607–619
47. Karami C, Taher MA (2019) A catechol biosensor based on immobilizing laccase to Fe3O4@ Au core-shell nanoparticles. Int J Biol Macromol 129:84–90

48. Karagoz B, Bayramoglu G, Altintas B, Bicak N, Arica MY (2011) Amine functional monodisperse microbeads via precipitation polymerization of *N*-vinyl formamide: immobilized laccase for benzidine based dyes degradation. Bioresour Technol 102(13):6783–6790
49. Xie J, Xu C, Kohler N, Hou Y, Sun S (2007) Controlled PEGylation of monodisperse Fe3O4 nanoparticles for reduced non-specific uptake by macrophage cells. Adv Mater 19(20):3163–3166
50. Park S-A, Jang E, Koh W-G, Kim B (2010) Fabrication and characterization of optical biosensors using polymer hydrogel microparticles and enzyme–quantum dot conjugates. Sens Actuators B Chem 150(1):120–125
51. Chai L, Zhou J, Feng H, Tang C, Huang Y, Qian Z (2015) Functionalized carbon quantum dots with dopamine for tyrosinase activity monitoring and inhibitor screening: in vitro and intracellular investigation. ACS Appl Mater Interfaces 7(42):23564–23574

Affiliations

Elham Arkan[1] · Changiz Karami[1] · Ronak Rafipur[2]

✉ Changiz Karami
Changiz.karami@gmail.com

[1] Nano Drug Delivery Research Center, Kermanshah University of Medical Sciences, Kermanshah, Iran

[2] Department of Chemistry, Faculty of Sciences, Azad University of Kermanshah, Kermanshah, Iran